Clay Minerals Do Not Influence Nitrous Oxide Production Via Denitrification in Simulated Oxygen Minimum Zones

A Thesis
Submitted to the Faculty
in partial fulfillment of the requirements for the degree of

Master of Science

in

Earth Science

by Luke Rein

Guarini School of Graduate and Advanced Studies
Dartmouth College
Hanover, New Hampshire

March 2026

Examining Committee

Mukul Sharma

Erich Osterberg

Wil Leavitt

George A. O'Toole

John F Kull, Ph.D.
Dean of the Guarini School of Graduate and Advanced Studies

Abstract

It has been proposed that export of organic carbon from the epipelagic zone to the seafloor can be increased by the addition of 20 mg L^{-1} of clay minerals to phytoplankton blooms. In natural environments, bacterial digestion of organic carbon sourced from phytoplankton blooms leads to the creation of oxygen minimum zones, where denitrifying marine bacteria produce nitrous oxide, a potent greenhouse gas. It is unknown if additional nitrous oxide results from the additional organic carbon transported to the seafloor via this method; therefore, a simulated oxygen minimum zone was developed that allowed us to measure the contribution of clay minerals to the production of nitrous oxide in oxygen minimum zone conditions. We developed an approach to test the influence of a proposed marine carbon capture and storage method on the production of nitrous oxide by denitrifying bacteria in the oxygen minimum zone. After purging the microcosms with helium to remove any gases save those produced by bacteria within the microcosm, then incubating microcosms containing representative marine bacteria and nutrients, we found that the addition of clay minerals did not change the amount of nitrous oxide produced via denitrification. This suggests that this method provides an effective means of increasing the transfer of organic carbon to the seafloor without risking additional greenhouse gas generation. Because the organic carbon found in phytoplankton blooms is primarily derived from atmospheric carbon dioxide, this method also provides a possible pathway to capture and sequester atmospheric carbon on a geologic timescale.

Preface

“The Sea, once it casts its spell, holds one in its net of wonder forever.”

– Jacques Yves Cousteau

Acknowledgements

Funding and support for this research was provided by John Simon Guggenheim Memorial Foundation, Astera Institute, Grantham Foundation, Schmidt Futures, and NASA award #80NSSC25M7042. Funding usage was reported to Dartmouth College chartstrings 20.469.368000.388951.0000.8161 and 20.469.582205.239572.1305.

The following individuals supported this experiment:

Annie Kandel: logistical support for field excursions and laboratory materials. Joshua Landis: laboratory support and maintenance. Diksha Sharma: guidance on N+N, NO_2^-, and DO measurements. Manasi Desai and David Fields: guidance, recipes, and nutrients for rearing *Calanus finmarchicus* and *Rhodomonas salina*. Vignesh Gokuladas Menon: guidance on bacterial filtration and 16S processing. Wil Leavitt: biological safety cabinets and growth nutrients. Jiawen Li, Carrie Harris, and Mia Thompson: guidance on procedures required to prepare media, measure bacterial growth, and sample growth medium. George O'Toole: growth medium. Shawna Pratt: guidance on bacterial counting. Isaiah Davidson: measured N+N and NO_2^-. Erich Osterberg: networking information for atmospheric scientists and academic advising. Emily Stuchiner: guidance on headspace gas sampling and ECD-GC. Lisa Martell and Rick Doucette: guidance on preparing samples. Michael Wyman: guidance on preparing growth medium. Marisa Palucis: academic advising and access to NASA funding. David Drapeau and the crew of *R/V Bowditch*: sample collections. Bailey Nordin: support for field excursions.

Table of Contents

List of Tables

List of Illustrations

Introduction

Clay minerals have been proposed as a method to capture and sequester atmospheric carbon dioxide, supported by evidence from brewing, wastewater, and environmental management industries. In brewing, bentonite clays are used to clarify beverages during fermentation by adsorbing to yeasts, proteins, and particulates that otherwise remain suspended in finished product (Sauvage et al. 2010; Pocock et al. 2011). Recent developments in wastewater treatment propose adoption of clay minerals to clarify water by adsorbing organic and inorganic pollutants prior to water release (Biswas et al. 2021; Shahzadi et al. 2025). On a larger scale, clays demonstrate ability to adsorb phytoplankton cells, a property useful in controlling phytoplankton blooms and mitigating the effects of red tide (Anderson 1997; Yu et al. 2023). These effects have also been investigated by our laboratory and others, where earlier work positively correlates clay addition with increased export of organic carbon from the epipelagic zone to the seafloor via increased flocculation of organic carbon and faster sinking rates of copepod fecal pellets (Sharma et al. 2024).

In natural ecosystems, zooplankton and marine bacteria remineralize nearly all of this sinking organic carbon before it reaches the seafloor, producing CO_2 (Hedges and Keil 1995; Honjo et al. 2008; Xie et al. 2019). Organic carbon may be sinking phytoplankton, TEP flocs, copepod fecal pellets, or other sinking biomass (Urban et al. 1993; Svensen et al. 2012; Liu and Wu 2016). In regions with very high primary productivity, such as upwellings found on western continental margins and the Arabian Sea, this remineralization depletes dissolved oxygen (DO) levels to

create an oxygen minimum zone (OMZ) where aerobic respiration is no longer possible (Bange et al. 2005; Bianchi et al. 2018). In these conditions, marine bacteria may abandon aerobic respiration in favor of alternative respiratory pathways as they digest organic carbon, including denitrification, where nitrate (NO_3^-) is reduced to nitrite (NO_2^-), nitric oxide (NO), nitrous oxide (N_2O), and eventually dinitrogen (N_2) by a series of reducing enzymes, and anaerobic ammonia oxidation (annamox), where NH_4^+ is oxidized by NO_2^- to form N_2 (Naqvi 1994; Ward et al. 2009; Thamdrup 2012; Wright et al. 2012; Van De Vossenberg et al. 2013) (Figure 1).

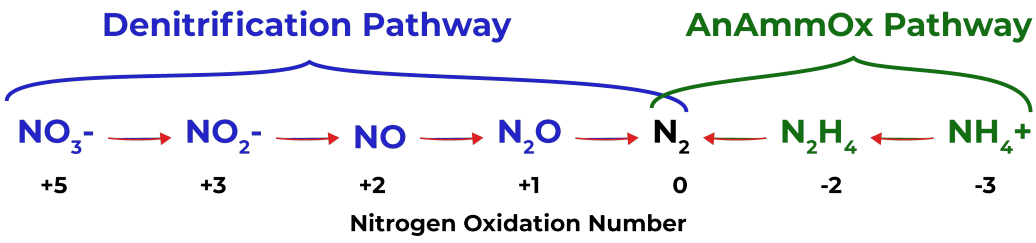

Figure 1: Nitrogen respiratory pathways investigated in this experiment. Modified from Kuypers et al. 2018.

Together, these two pathways account for the majority of fixed nitrogen loss in marine environments (Lam and Kuypers 2011; Xu et al. 2025). For denitrifying bacteria, not all reduction steps take place, with about a third of bacteria lacking genes required to encode nitrous oxide reductase (nosZ), or failing to express it due to environmental factors (Philippot et al. 2011). While anammox does not significantly impact atmospheric gas balances, denitrification accounts for the largest marine source of nitrous oxide to the atmosphere, making up about 25% of all natural N_2O release with 4 teragrams (Tg) per year (yr^{-1}) (Kuypers et al. 2018).

The potency of N_2O as a greenhouse gas and its long atmospheric residence time provide significant climate risks. (Ravishankara et al. 2009; IPCC 2022). Because of the demonstrated interdependency between organic carbon digestion and incomplete denitrification and the global warming effect of N_2O, the effects of clay mineral addition to organic-carbon rich ocean conditions warrants careful study.

Of particular interest is the possibility that clay addition and the ensuing flocculation of organic carbon promotes anammox rather than denitrification. Although oxygen concentrations as low as 1.2 μM may limit anammox, sinking particles can reach complete anoxia possibly providing a microenvironment that favors anammox over denitrification (Woebken et al. 2007; Bianchi et al. 2018). or enough ammonium that anammox becomes more favorable in waters enriched in NO_2^- produced by denitrification (Kalvelage et al. 2011; Karthäuser et al. 2021). Evidence of anammox-supporting microsites in sinking particles suggest that the addition of clay to ocean waters may not only increase the net export of carbon from the epipelagic to the seafloor, but also foster conditions ideal for anammox, providing an alternative pathway to complete reduction of nitrogen ending in N_2 generation instead of the long-lived ozone depleting byproducts of incomplete denitrification.

To investigate whether clay minerals promote anammox in OMZ conditions, we designed an experiment replicating the high nutrient, low oxygen conditions resulting from a phytoplankton bloom and tested if the addition of clay minerals decreases the amount of N_2O released. Due to the previously observed effects of clay particles promoting anammox, we hypothesized that 20 mg L^{-1} clay treatment

will result in a lower concentration of N_2O in the headspace gases of the microcosms, measured via electron capture detector gas chromatography (ECD GC). Relative contributions of denitrification and anammox to N_2 and N_2O in the headspace were facilitated by using a ^{15}N enriched NH_4^+ to differentiate whether headspace gases were sourced from NO_3^- or NH_4^+ using isotope ratio mass spectroscopy (IRMS). Microcosms were filled with sterile, deoxygenated growth media and then flushed with helium to remove nitrogen species form the headspace prior to the start of the experiment. After inoculation with copepod fecal pellets, microcosms were incubated for 48 hours and periodically sampled to observe evolution of nitrogen species. This method allowed us to compare changes in the nitrogen cycle between experimental treatments; none were observed.

Materials & Methods

Seawater collection

To prepare growth media and provide aquaria water for phytoplankton and zooplankton, seawater was collected from the Gulf of Maine and filtered through 0.2µm PES filter cartridges (AcroPak 500, part number 12991) into acid-washed 20L HDPE jugs. This filtered seawater (FSW) was stored at 4°C until used for media preparation or to replenish aquaria for sample organisms.

Phytoplankton rearing

Phytoplankton (*Rhodomonas salina*) stocks were maintained using L1 medium prepared from autoclaved 0.2 µm FSW and stock solutions purchased from the National Center for Marine Algae & Microbiota (MKL150L) or F/2 Algae Food

purchased from Fritz Aquatics (84100 and 84101) and amended with additional trace metals and vitamins from the NCMA stock media kit.

Zooplankton Collection and Rearing

Copepods (*Calanus finmarchicus*) were collected from the Gulf of Maine during August 2024 and June 2025 using a plankton net on board the *R/V Bowditch*. Nets were towed at the surface and the cod end emptied into buckets of seawater collected from 20 to 40 meters depth. Individual *Calanus* were hand-dipped from the collection buckets and transported to a walk-in refrigerator in 3L jars packed in ice shavings. Captive *Calanus* were fed the laboratory-reared *Rhodomonas salina*, their aquaria water was periodically exchanged with new FSW, and fecal pellets removed every two to three weeks. Each jar contained about 45 *Calanus* when captured, and two to three *Calanus* per jar expired each week of captivity.

Developing an experimental medium

Initial experiments were performed using 1000mL media bottles containing 0.2µm FSW inoculated with a blend of fresh and freeze-dried *Calanus* fecal pellets. These bottles were wrapped in aluminum foil to prevent photosynthesis and kept inside a Coy glovebox (O_2 concentration approximately 160 ppm) to encourage deoxygenation. These experiments consistently demonstrated DO levels below 15 µM, low enough to encourage denitrification. OD600 measurements increased and NO_3^- levels decreased throughout the experiment, indicating bacterial growth and their ability to facultatively consume NO_3^- once DO levels had become depleted (Figure 2).

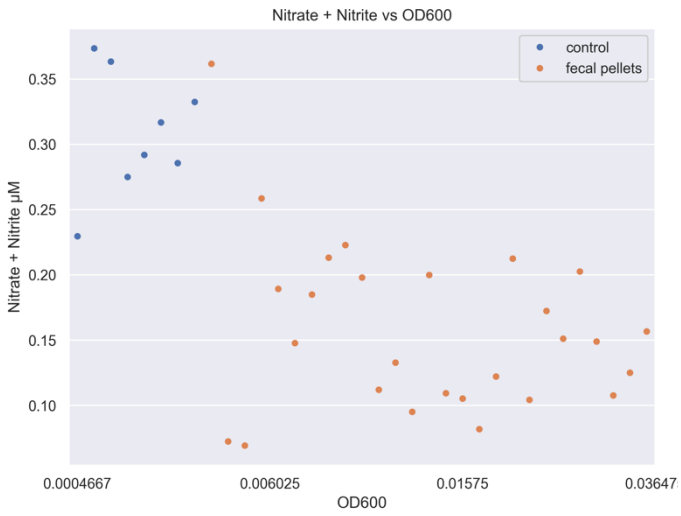

Figure 2

Demonstrates the relationship between higher bacterial counts measured by OD600 and decreasing N+N measurements in a preliminary experiment. These observations, along with DO less than 15 µM, informed us that fecal pellets contained facultative anaerobes and could serve as a source of bacteria for this experiment.

This finding suggested that in low oxygen environments, bacteria present in *Calanus* fecal pellets facultatively employed denitrification to continue digestion of organic carbon provided by the fecal pellets. However, these large bottles did not provide the ability to measure gases generated in the microcosms, and furthermore were susceptible to biological contamination inside the glovebox and introduced by the sampling procedure. Therefore, changes were made to the experimental protocol. Sealed 200 mL serum bottles were employed, which allowed for the anaerobic preparation of aseptic media, sterile inoculation and sample withdrawal, and maintenance of a sealed, pressurized headspace to reliably sample N_2O. 200 mL sample bottles (Kimble 61000G-200) were sealed with butyl rubber stoppers (ChemGlass CLS-4209-14) and crimped shut with aluminum closures (Wheaton 224193-06). These containers were tested and found to hold pressure up to 40 PSI for over a month even after the stoppers had been sampled through several times.

Recipe	NO_3^-	NO_2^-	NH_4^+	Total N	Acetate	Total OC	DO
OMZ	**35**	**6**	**2**	**43**		**10**	**<15**
90404				154091		235615	<5
Tryptic Soy Broth				194189		83261	<5
Wyman ASW +	1870		18695	24580	24380	26142	<5
Wyman ASW	5883		18695	24578	12190	12190	<5
Wyman Lite	**35**	**0.15**	**73**	**110**	**49**	**60**	**<5**

Table 1: Comparison of OMZ conditions to growth media. While richer growth media could be used to culture fecal pellets microbiomes, inoculations from these cultures did not grow in conditions that replicated the OMZ, so a diluted medium (Wyman Lite) was used for this experiment. Concentrations are in µmoles per liter *(Devol and Hartnett 2001; Lam et al. 2009; Wyman et al. 2013; Bristow et al. 2016; Cavan et al. 2017)*.

Media selection

Based on the evidence of denitrification in FSW amended only with fecal pellets, several growth media recipes were tested (Table 1). Early iterations of media selection using commercially available broths (Millipore 90404 and BD BBL Trypticase Soy Agar 211043) were chosen to ensure adequate nutrients for bacterial growth, utilizing a chemical reductant (sodium thioglycolate) to scavenge residual DO from growth media and resazurin to act as a colorimetric indicator of oxygen presence (Burd 2020). After bacterial growth was observed via increases in NO_2^- and OD600, an amended seawater media following a description by Wyman et al. was tested and yielded similar results (Wyman et al. 2013). After we determined that media can be effectively deoxygenated by boiling, thioglycolate and resazurin were removed from subsequent media recipes and representative DO measurements were made with the Winkler method to confirm low oxygen levels in experimental media. Removal of thioglycolate and resazurin from final media formulations reduced potential interference with carbon and nitrogen levels in

media, and the possibility of thioglycolate, a reductant, artificially reducing NO_3^- to NO_2^- and obscuring signals of denitrification. Finally, this media was adapted to reflect NO_3^- concentrations in the Arabian Sea, the site of regular, well documented phytoplankton blooms and a persistent OMZ, and the concentration of other nutrients was scaled in proportion to the original recipe (Morrison et al. 1999; Wyman et al. 2013).

Sampling Protocol Development

To quantify and compare N_2O production with and without clay, measurement of N_2O in headspace gas was performed by electron capture detection gas chromatography (ECD GC), a technique capable of measuring N_2O concentrations at the parts per billion level. A β particle source is used to excite the gas sample, and the resulting electrons released from the gas sample are measured (Wentworth and Chen 1967; Wentworth et al. 1971; Wentworth and Freeman 1973; Cohen 1977) Additionally, to determine the pathway producing the nitrogen species in the headspace, isotopic tagging was used to differentiate between two source nitrogen pools. NO_3^-, which is reduced by denitrification, was prepared using $NaNO_3$ (VWR CA71008-746), while NH_4^+, the substrate for anammox, was prepared using $^{15}NH_4^+Cl$ (Sigma-Aldrich 299251) with ≥98% ^{15}N. If N_2 is produced via anammox, the $\delta^{15}N$ measurement in the headspace N_2 will be enriched relative to the control treatments, whereas if denitrification is the predominant pathway for N_2, $\delta^{15}N$ will be depleted compared to the control treatments. To facilitate this measurement, ultra high purity (UHP) helium (Table 2), NO_3^- + NO_2^- instead of dinitrogen or

argon, was employed as a headspace flushing gas to avoid interfering with IRMS measurements (Doucett, personal communication).

UHP Helium Elemental Composition			
Gas	**ppm**	**k (mol/kg*bar)**	**Gas solubility (mol/L)**
He	999990	0.00038	7.85E-04
N_2O	≤ 2	0.025	1.03E-07
N_2	5	0.00065	6.71E-09
O2	1	0.0013	2.68E-09
CO2	1	0.034	7.02E-08
CO	1	0.00099	2.04E-09

Table 2: Elemental makeup of ultra high putriy helium. Henry's constants and expected solubility of that gas under experimental conditions are included based on maximum possible concentrations of gases. ECD-GC measurement of N_2O suggests that N_2O concentrations in this gas are closer to 0.08 ppm.

Inoculant preparation

Fecal pellets were collected from Gulf of Maine wild-caught *Calanus finmarchicus* that were subsequently reared in laboratory aquaria (3L glass jars) stored in the dark at 4° C on a diet of *Rhodomonas salina.* We collected fecal pellets with a turkey baster and filtered them through 52 µm nylon mesh, then rinsed the pellets with 0.2µm FSW, and centrifuged the pellets at 3000x*g* for 2 minutes in 50 mL centrifuge tubes. The centrifuged pellets were resuspended by vortexing in 100 mL 0.2µm FSW inside a sealed 200 mL serum bottle for 30 seconds, then bubbled with UHP helium for 15 minutes, cooled in a refrigerator, then bubbled with UHP helium for an additional 15 minutes to strip remaining oxygen from the inoculant. Inoculant was stored in the refrigerator until it was used.

Media preparation

0.2µm FSW was amended by diluting gravimetrically prepared stock solutions. $^{15}NH_4^+Cl$ (13,310,600 ‰ enriched relative to natural abundance) was used to isotopically tag the NH_4^+ stock solution. Following nutrient amendment, the

seawater was degassed by boiling on a hot plate set to 350 °C for 75 minutes. Degassed seawater was immediately poured into 200 mL serum bottles and capped with rubber septum stopper pierced with a 21 gauge stainless steel needle. The needle allowed any air to be expelled from the bottle, and when the needle was removed, resulted in a completely filled bottle with zero headspace.

While still warm, 50 mL of media was withdrawn using an autoclaved syringe to create 50 mL of headspace while the bottle was being pressurized with UHP helium. The remaining media was bubbled with UHP helium for 15 minutes and pressurized to 16 PSI. Tests of the oxygen content at this point indicated DO levels of 13.4 ± 2.2 μM, and were comparable to the OMZs that our microcosms were intended to replicate (Bange et al. 2005; Paulmier and Ruiz-Pino 2009). Bottles were chilled overnight in a refrigerator, then bubbled again with UHP helium for 15 minutes and pressurized to 16 PSI. Bottles were randomly assigned to an experimental group. Three bottles were assigned to the baseline group, and 15 bottles each were assigned to a Fecal Pellet (FP), Fecal Pellet + Clay (FPC), or Clay (C) treatment (Figure 3).

Clay preparation

A sterile mixture of palygorskite and nontronite clays (approximately 4:1 ratio) was sonicated in MilliQ water to produce a 4 mg/mL suspension and stored at room temperature until inoculation following the protocols used to test the effects of these clay minerals on organoclay flocculation (Sharma et al. 2024)

Inoculation

Microcosms were inoculated with a sterile syringe (BD 309657) with 21 gauge stainless steel needle (BD 305165) through the septum lid (Figures 3 and 4). Microcosms were inoculated in order of sampling time, i.e., 0 hour microcosms, then 6 hour microcosms, then 12 hour microcosms, etc. All inoculations were completed prior to taking T = 0 measurements.

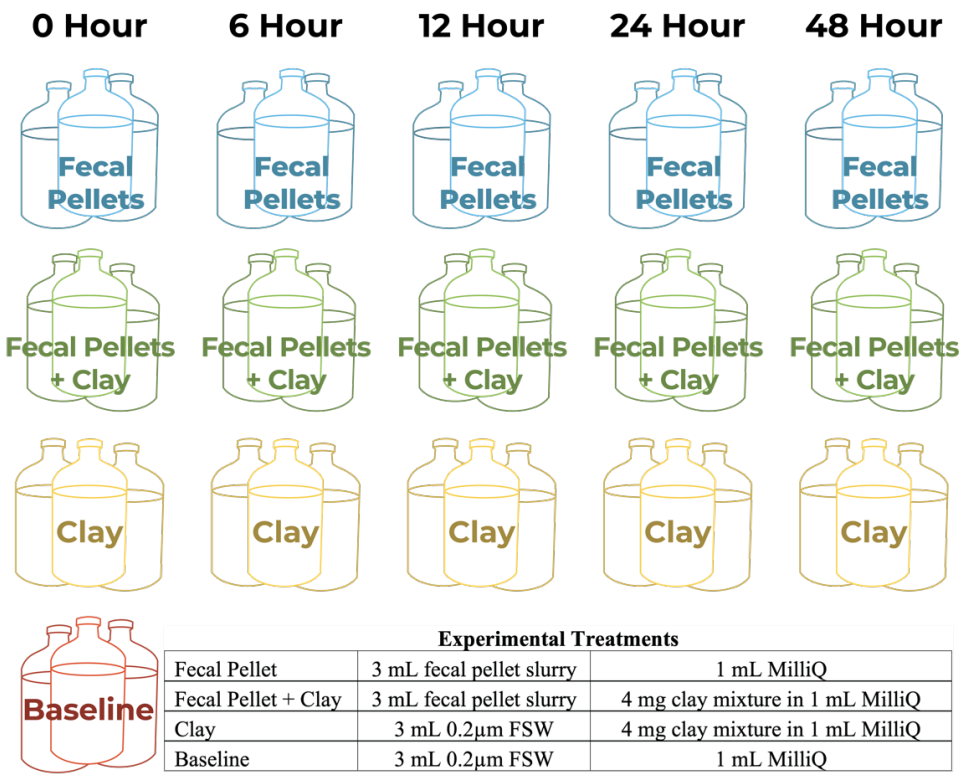

Experimental Treatments

Fecal Pellet	3 mL fecal pellet slurry	1 mL MilliQ
Fecal Pellet + Clay	3 mL fecal pellet slurry	4 mg clay mixture in 1 mL MilliQ
Clay	3 mL 0.2µm FSW	4 mg clay mixture in 1 mL MilliQ
Baseline	3 mL 0.2µm FSW	1 mL MilliQ

Figure 3: Experimental treatment overview.

Measurements

As demonstrated in Figure 4, two 20 mL gas samples were withdrawn from the headspace of the microcosm using a 25 mL Hamilton gas syringe (Hamilton 1025SL) with a 25 gauge stainless steel needle (BD 305125) and stored in 12 mL evacuated soda glass vials (Exetainer E2853). The first sample was sent to Cary

Institute of Ecosystem Studies for N_2O concentration analysis using ECD GC and the second sample was sent to UC Davis Stable Isotope Facility for isotopic analysis using IRMS. Liquid samples were withdrawn from microcosms using sterilized 50 mL syringes (BD 309653) and 21 gauge stainless steel needles (BD 305165). 35

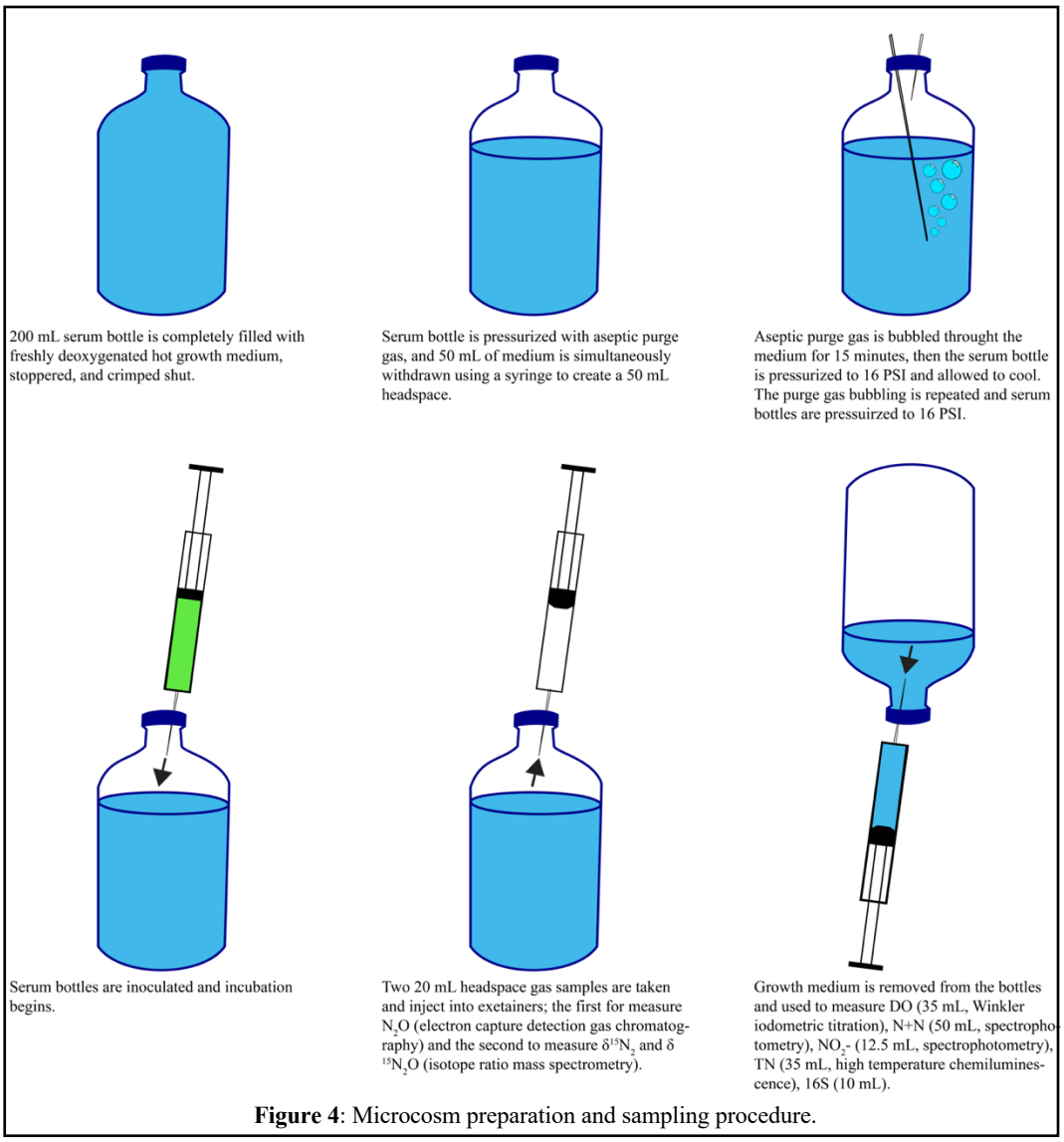

Figure 4: Microcosm preparation and sampling procedure.

mL of sample was taken for DO analysis using the Winkler method adapted for use with a 25 mL sample volume. 50 mL of sample was taken for combined NO_3^- + NO_2^- (N+N) analysis and 12.5 mL of sample was taken for NO_2^- analysis. Both

samples were measured according to standard spectrophotometric methods (Hansen and Koroleff 1999). The N+N sample was diluted to 20% strength using MilliQ water, then passed through a cadmium granule/copper sulfate reducing column to reduce NO_3^- to NO_2^-. Then sulfanilamide and NEDA were added to the samples, producing an aniline dye from the NO_2^-, which was measured for absorbance at 543 nm with a Shimadzu UV-1900i Plus spectrophotometer. Measured absorbances were compared to standard solutions of 0, 2, 5, and 10 µM strength. 10 mL of liquid sample was taken and frozen at -25°C for 16S analysis. These samples have not yet been analyzed. Finally, 30 to 40 mL of sample was taken for total nitrogen (TN) and dissolved organic carbon (DOC) analysis using a Shimadzu TOC/TNM chemiluminescent analyzer. TN and DOC samples were analyzed using either 5 or 8 measurements of the same sample, and peak areas were compared to a calibration curve of 280.0, 700.1, and 2800.0 µg/L for nitrogen and 600, 1200, and 2400 µg/L for carbon. Sample batches were processed according to best practices outlined in Halewood et al. (Halewood et al. 2022).

Statistical Analysis

We compared mean data for each treatment with ANOVA, Student's, or Welch's T-tests as appropriate, using functions included in Microsoft Excel's (16.66.1) Data Analysis tools to determine differences between treatments (See Table 3). The following python (3.12.2) libraries were used for data analysis and plotting: seaborn (0.13.2), pandas (2.21), numpy (1.26.4), and matplotlib (3.8.3)

Results

We began analysis by comparing the two methods used to measure N_2O because this measurement is central to answering our hypothesis of whether clay minerals reduce the production of N_2O in OMZs (Figure 5). The slope of the linear regression is almost 1 (m = 0.984), although the y intercept of 66 ppb indicates a systematic bias between the two measurements, with the IRMS method over-measuring N2O concentration. Because the ECD-GC is specifically designed to report accurate and precise N2O concentration data, we will use the ECD-GC data for analysis in this report.

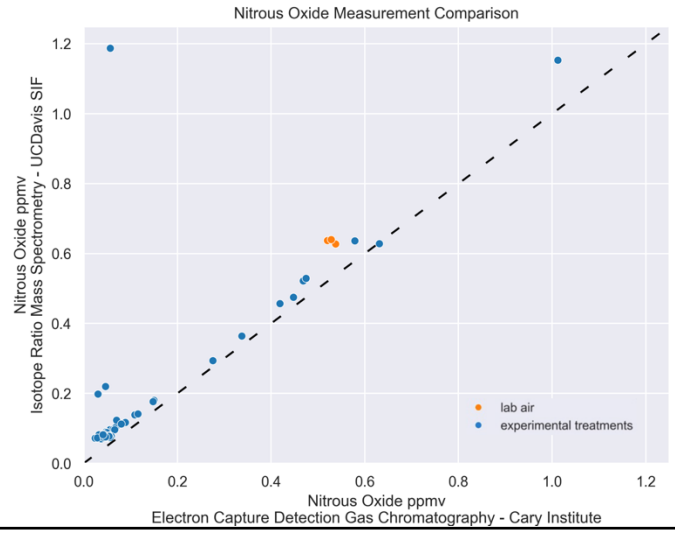

Figure 5: N_2O measured by two unrelated laboratories using different techniques. Black dashed line has a slope of 1.000 and y-intercept of 0.0. If data were perfectly correlated, they would plot on this line. Instead, measurements made using IRMS were systematically higher than those made using ECD-GC and data points plot above this line. ECD-GC measurements were used for analysis in this experiment.

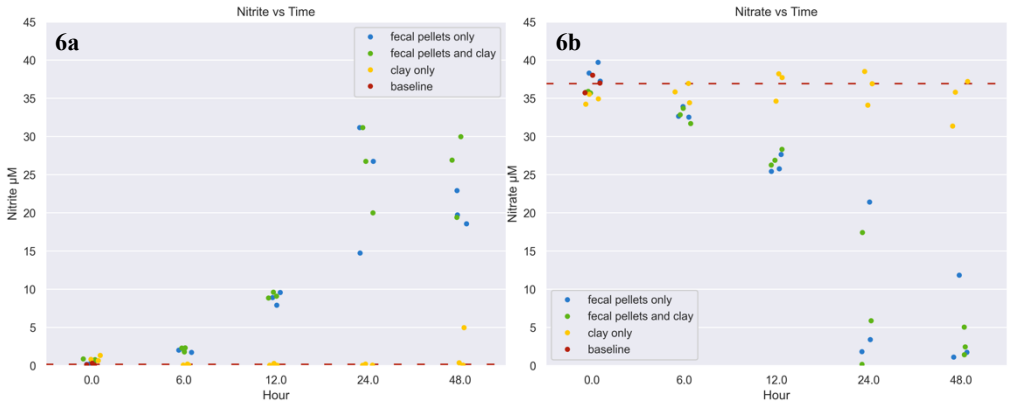

Figure 6a: NO_2^- measurements, indicating denitrification by increase in NO_2^- concentration.
Figure 6b: NO_3^- measurements, indicating denitrification by decrease in NO_3^- concentration.

Measurements of NO_2^- provided evidence of denitrification in experimental treatments with fecal pellets, supported earlier observations that fecal pellet inoculations contain bacteria capable of denitrification, and therefore, production of N_2O (Figure 6a).

Beginning at t = 6 hours, both FP and FPC treatments differed significantly from the clay treatments, but were not different from each other via T test ($\alpha = 0.05$, n = 3, Student's T-test if variance was equal or Welch's if variance was not equal). Full statistics are shown in Table 3. NO_3^- exhibited the decreasing trend with time observed in preliminary experiments (Figure 6b). At T = 0, all experimental treatments are statistically equal, while any measurements made later indicate that the experimental treatments are not equal. Except for the measurement made at T = 12, FP and FPC treatments were indistinguishable by their NO_3^- measurements.

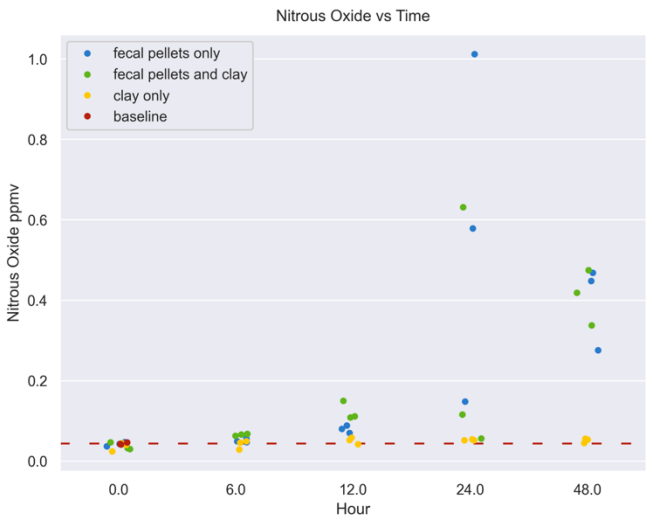

Figure 7: N_2O production is clearly visible in fecal pellets treatments. At T = 6 and T = 12, the FCP treatments have statistically higher N_2O than their FP counterparts; this is no longer true at later timepoints.

ANOVA										
Hour	**0**		**6**		**12**		**24**		**48**	
	f	**f_{crit}**	**f**	**f_{crit}**	**f**	**f_{crit}**	**f**	**f_{crit}**	**f**	**f_{crit}**
NO_2	10.28	4.07	92.92	5.14	270.15	5.14	18.14	5.14	33.14	5.14
N+N	5.62	4.07	0.74	5.14	2.10	5.14	0.98	5.14	2.57	5.14
N_2O	0.77	4.07	8.83	5.14	17.41	5.14	2.20	5.14	23.32	5.14
T test										
Hour	**0**		**6**		**12**		**24**		**48**	
type	**Student's**		**Welch's**		**Welch's**		**Student's**		**Welch's**	
	t	**1 tail t_{crit}**	**t**	**1 tail t_{crit}**	**t**	**1 tail t_{crit}**	**t**	**1 tail t_{crit}**	**t**	**1 tail t_{crit}**
NO_2	-5.202	2.132	-1.328	2.353	-0.730	2.353	-0.298	2.132	-1.479	2.353
	Welch's		**Student's**		**Student's**		**Student's**		**Student's**	
N+N	3.200	2.920	0.041	2.132	-2.545	2.132	-0.096	2.132	-0.492	2.132
	Student's		**Student's**		**Welch's**		**Student's**		**Student's**	
N_2O	0.998	2.132	-4.861	2.132	-3.049	2.353	1.009	2.132	-0.178	2.132

Table 3a: Statistics of analysis of NO_2^-, N+N, and N2O in microcosms. Significant results ($\alpha = 0.05$) are highlighted in green.

ANOVA										
Hour	**0**		**6**		**12**		**24**		**48**	
	f	**f_{crit}**	**f**	**f_{crit}**	**f**	**f_{crit}**	**f**	**f_{crit}**	**f**	**f_{crit}**
$\delta^{15}N_2$	3.419	4.066	4.566	5.143	6.131	5.143	13.386	5.143	4.348	5.143
$\delta^{15}N_2O$	3.998	4.066	1.217	5.143	17.117	5.143	45.851	5.143	21.161	5.143
T test										
Hour	**0**		**6**		**12**		**24**		**48**	
type	**Welch's**		**Student's**		**Welch's**		**Student's**		**Student's**	
	t stat	**1 tail t_{crit}**	**t stat**	**1 tail t_{crit}**	**t stat**	**1 tail t_{crit}**	**t stat**	**1 tail t_{crit}**	**t stat**	**1 tail t_{crit}**
$\delta^{15}N_2$	0.592	2.920	0.518	2.132	2.112	2.353	3.482	2.132	5.734	2.132
	Welch's		**Welch's**		**Student's**		**Student's**		**Welch's**	
$\delta^{15}N_2O$	-1.984	2.920	2.014	2.920	0.902	2.132	-2.196	2.132	-0.335	2.920

Table 3b: Statistics of analysis of $\delta^{15}N_2$ and $\delta^{15}N_2O$ in microcosms. Significant results ($\alpha = 0.05$) are highlighted in green.

N_2O measurements (Figure 7) exhibit clear evidence of denitrification. At T = 6 and T = 12, FP and FPC treatments can be differentiated with FPC having higher N_2O concentrations; this cannot be observed in later measurements. At T = 24 and T = 48, there is no statistical difference between either the FP or FPC treatments, although the variance of the T = 24 measurements is much greater. N_2O and NO_2^- measurements across all measurements were somewhat correlated, with a r-squared value of 0.610. $\delta^{15}N_2O$ data illustrated clear differences in the source of N_2O in microcosm headspaces. All microcosms exhibited relatively heavy $\delta^{15}N_2O$ at the

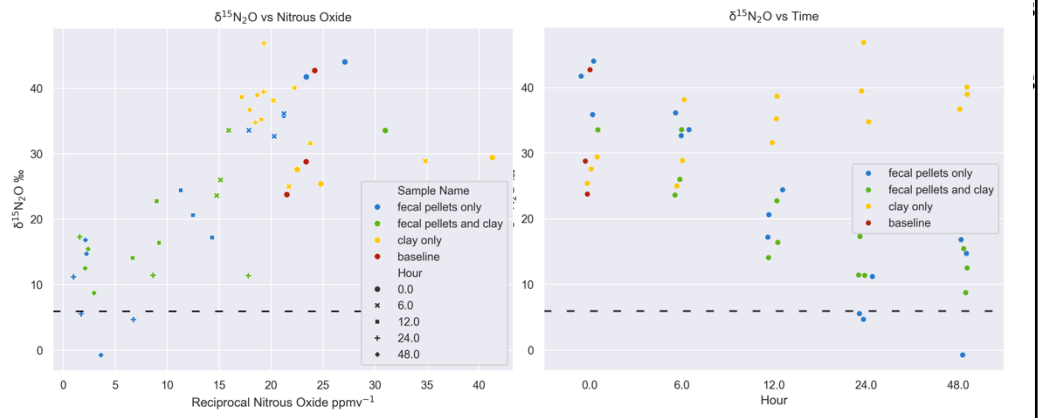

Figure 8: $\delta^{15}N_2O$ reveals denitrification as the source of N_2O. Low $\delta^{15}N_2O$ in microcosms inoculated with fecal pellets indicated that N_2O is produced by bacteria preferentially using ^{14}N for a denitrification substrate, indicated by the inverse relationship between $\delta^{15}N_2O$ and N_2O concentration (8a). When plotted against time, rising $\delta^{15}N_2O$ in clay microcosms suggested that a reservoir of $^{15}N_2O$ in the growth medium is equilibrating into the headspace in the microcosm (8b). The dashed line indicates $\delta^{15}N_2O$ of laboratory air, $\delta^{15}N_2O$ values are in reference to atmospheric standards.

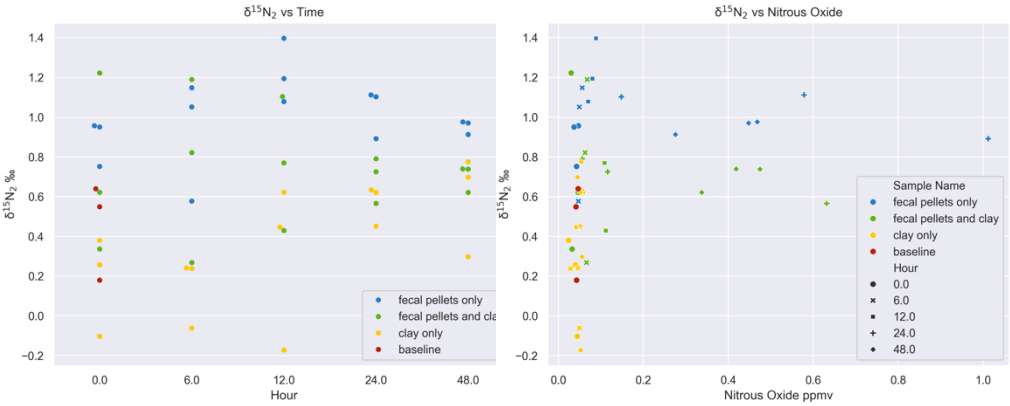

Figure 9: $\delta^{15}N_2$ measurements did not display evidence of anammox. Across the duration of the experiment, treatments exhibited no statistically significant slope, but were statistically different between experimental groups (9a). When plotted against N_2O, $\delta^{15}N_2$ did not exhibit relationships (9b). $\delta^{15}N_2$ values are in reference to atmospheric standards.

$\delta^{15}N_2$ data did not exhibit clear trends aligning with other metrics, but experimental treatments were distinguishable from each other (Figure 9).

Discussion

N_2O Concentrations Reject Hypothesis of Diminished Denitrification.

As observed in earlier experiments, decreasing N+N and rising NO_2^- concentrations with time support the hypothesis that denitrification activity is occurring in microcosms containing fecal pellets. This hypothesis is further supported by the N_2O measurements via ECD GC and IRMS, which both demonstrate production of N_2O (Figure 7).

After 12 hours, N_2O concentrations in the FP treatments and FPC treatments were indistinguishable using a t-test ($\alpha = 0.05$), disproving our hypothesis that the addition of clay minerals to these OMZ microcosms decreases the concentration of N_2O produced. At the 6 and 12 hour timepoints, we observed a statistically significant different ($\alpha = 0.05$) in the mean N_2O measurements between FP and FPC treatments, with N_2O in treatments with clay exceeding those without. These findings suggests that the introduction of clay has kinetic effects on denitrification, but ultimately does not increase the amount of denitrification. Because clay has been shown to increase the settling rate of sinking organic particles, either by increases in density or promoting formation of larger flocs, this action may push N_2O production deeper into the ocean, thereby increasing the time this greenhouse gas remains dissolved and allowing more time for complete denitrification and full reduction to N_2, or simply increasing the residence time of N_2O in the ocean.

N_2O concentrations reject hypothesis of diminished denitrification

Concentrations of NO_2^- were indistinguishable between FP and FPC treatments. This finding further suggests that denitrification is not affected by the presence of clay, although this observation does not agree with the N_2O data that show greater N_2O production occurring quickly in clay-amended microcosms (Figure 7). A possible reconciliation of this apparent disagreement is that the presence of clay diminishes complete denitrification early, or the presence of clay promotes complete denitrification to N_2 later than a non-clay treatment does.

Isotopic evidence of incomplete denitrification and anammox

$\delta^{15}N_2O$ data provided additional evidence of incomplete denitrification where NO_3^- is not completely reduced to N_2 gas (Figure 8). Treatments that exhibited greater N_2O concentrations also exhibited lower $\delta^{15}N_2O$ measurements; when $\delta^{15}N_2O$ data were plotted against the reciprocal of N_2O data obtained by ECD GC, a positive correlation is clearly observed between these values. Plotting a linear equation to these data (r squared = 0.530) suggests that the gas mixture in the headspace is the result of mixing between two endmember sources of N_2O: one abiogenic source that was initially present prior to inoculation, and one completely biogenic source expected if all available NO_3^- were denitrified to N_2O. While a weak positive correlation (r squared = 0.257) was observed between the concentration of headspace N_2O and time in abiotic treatments, plotting the $\delta^{15}N_2O$ of abiotic treatments against time yielded a stronger correlation (r squared = 0.402) that suggested that any N_2O that remained in the microcosms after purging must be relatively heavy. IRMS measurement of the UHP helium purge gas indicated that

it was lighter ($\delta^{15}N_2O$ = 19.2 ‰) than the abiotic baseline or clay treatments; this observation suggests that an abiotic conversion of $^{15}NH_4^+$ to $^{15}N_2O$ occurred during the sterilization and degassing procedure and was subsequently recorded by these $\delta^{15}N_2O$ measurements. IRMS data additionally confirm that N_2O measured in the biological treatments is produced via denitrification, as bacteria preferentially utilize the lighter ^{14}N as a substrate to decrease energy required to respire. Thus, we surmise that the mixing of these two endmember reservoirs of N_2O produced the trend observed in the data (Figure 8b).

Elevated $\delta^{15}N_2$ measurements are an indicator of N_2 generated via the anammox pathway. $\delta^{15}N_2$ data measured here are indistinguishable from atmospheric $\delta^{15}N_2$ levels, indicating an error in the sampling protocol that introduced atmospheric N_2, a leak in the exetainers used for sample transfer, or absence of measurable anammox in this experiment. Despite the loss of up to 90% of the $^{15}NH_4^+$ during media preparation, we still expected anammoxogenic N_2 to reflect the high ^{15}N enrichment (13,310,600 ‰) available to anammox bacteria. Therefore, the lack of signal can be interpreted in one of two ways: that clay addition does not increase anammox rates in OMZ systems, or that measurement and sampling errors prevent us from measuring $\delta^{15}N_2$. Because the samples for $\delta^{15}N_2$ were taken from the same samples used to measure $\delta^{15}N_2O$, and these $\delta^{15}N_2O$ measurements indicate denitrification activity, we consider that the $\delta^{15}N_2$ indicate no measurable anammox in the system.

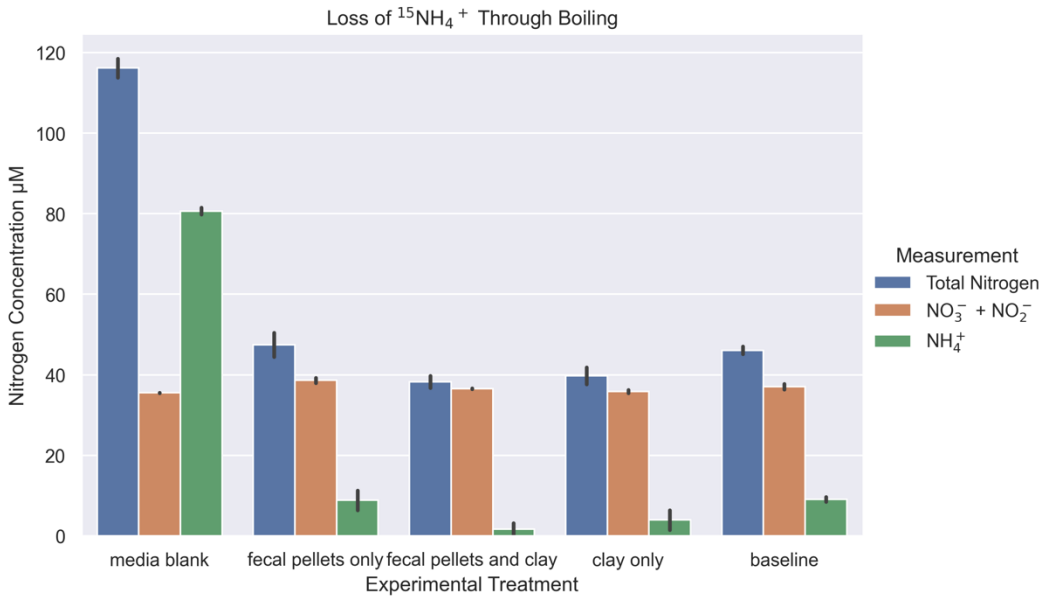

Figure 10: Loss of NH_4^+ during the deoxygenation process. This depleted the reservoir of available $15NH_4^+$ to track annamox, but the high $\delta^{15}N$ enrichment of the NH_4^+ pool, about 13,000,000 ‰, should allow any measurable $^{15}N_2$ resulting from anammox to be measurable by IRMS.

Total Nitrogen and Loss of $^{15}NH_4^+$

A decrease in total nitrogen (TN) was observed relative to the initial medium blank as prepared, with a mean nitrogen loss of 80.3 ± 4.6 µM in experimental microcosms when compared to the blank (Figure 10). Because N+N measurements made in the microcosms at T = 0 indicated relatively small changes in NO_3^- and NO_2^- in the microcosms (0.9 ± 1.2 µM greater than measurements of the growth medium as prepared), we determined that the TN lost from the microcosms was due to the loss of $^{15}NH_4^+$. In earlier experiments where TN was only measured after inoculations with bacteria and $\delta^{15}N_2$ was not measured, we believed that the loss of TN was due to anammox occurring rapidly in microcosms rich in $NH4^+$ and NO_2^-. Here, we observed the loss of $^{15}NH_4^+$ in abiotic conditions during this experiment and the absence of any measurable $\delta^{15}N_2$. These observations prompted us to take TN measurements of the growth medium after deoxygenation and before

inoculation and draw the conclusion that the loss of the $^{15}NH_4^+$ occurred during the boiling process used to deoxygenate the growth medium. We determined that degassing the growth medium by rolling boil on a hotplate, rather than steam boiling inside an autoclave, was most likely responsible for the difference in NH_4^+ concentrations between the prepared medium and the medium as inoculated, as this was a point where our media preparation protocol diverged from the protocol we had followed prior to this point. It is likely that the bubbles produced by a rolling boil on a hotplate, as observed in other degassing protocols, rather than the simmering boil inside an open-topped autoclave, led to the loss of some nitrogen from both the NO_3^- and $^{15}NH_4^+$ pools, but removed approximately 93% of the $^{15}NH_4^+$ (79.9 ± 2.7 μM) compared to an initial concentration of 86.0 ± 5.0 μM.

Variability in the N+N

The slightly more elevated and varied N+N measurements in experimental treatments may be due to inequal breakup of solid fecal pellets while vortexing inoculant; while sonicating produces a more homogenous inoculant, it does so at the risk of lysing bacteria in the inoculant and was therefore avoided.

Winkler Method Limitations

During these experiments, DO concentrations obtained by the Winkler method exceeded maximum oxygen dissolution levels possible to observe in seawater. Because previous iterations of this experiment had not exhibited such fluctuations, and tests of the Winkler reagents with known low-oxygen media indicated that the reagents were working correctly, we determined that these measurements must be spurious. Later research indicated that in very high NO_2^- conditions, the NO_2^- can

interfere with the final titration of iodine to iodide and yield an artificially elevated DO level. This can be mitigated either by using a sodium iodide azide reagent instead of a sodium iodide reagent, or by the use of an oxygen sensor (Barnett 1939; Rounds et al. 2013). Either method is suitable for ongoing experiments, but a properly calibrated oxygen probe also saves many hours of measuring time and enables a larger sample size.

N_2O Measurement

Many N_2O measurements were below the ECD-GC's lowest standard comparison of 0.25 ppm. These data have been included in the study because their presence does indicate that N_2O concentrations in these experimental treatments are not above 0.25 ppm.

The helium blanks tested by two different laboratories using two different methods both yielded N_2O concentrations around 0.08 ppm, about twice the lowest measurements observed in experimental treatments. The UHP helium gas used for purging the microcosms does contain impurities which may be inconsequential for most industrial uses but appear to make a true zero measurement of N_2O impossible. Based on data provided by AirGas, UHP helium may contain up to 1 ppm N_2 and 2 ppm N_2O (Table 2), although our measurement of the UHP helium blanks suggest that the N_2O quantity is lower. The lower N_2O measured in the microcosm headspace relative to the UHP blank is most likely due to N_2O's higher solubility than helium; about twice as much at the conditions studied here. This observation is supported by the N_2O concentrations at T = 0 and in clay measurements of about half the UHP helium blank's N_2O measurement.

Maximum N_2O and N_2 Production

To provide a simplistic model of maximum N_2 and N_2O production, we assume that anammox and denitrification can occur completely, that denitrification is limited by the amount of NO_3^- initially present as an oxidizer, and that anammox will be limited by the amount of NH_4^+ available to combine with NO_2^- produced by denitrification. Assuming only denitrification, the 7.06 μmoles of NO_3^- in each microcosm can produce 3.53 μmoles of N_2O (incomplete denitrification), 3.53 μmoles of N_2 (complete denitrification), or some mixture of the two. Assuming denitrification and anammox occur simultaneously to provide the NO_2^- that anammox needs, the 1.81 μmoles of NH_4^+ in each microcosm produces up to 1.81 μmoles of N_2 per microcosm. Because anammoxogenic N_2 is sourced from a combination of $^{15}NH_4^+$ and $^{14}NO_2^-$, it is expected that this N_2 is isotopically enriched, but calculating the level of enrichment depends on factors that we are unable to measure.

ANOVA tests indicate that there are no significant differences in the amount of N_2O created in microcosms treated with fecal pellets and those not treated with fecal pellets ($p = 0.05$). We cannot distinguish between the N_2O produced by microcosms with or without clay at any of the time points by using a t test; therefore, we can say that there is no statistical difference between N_2O production in environments where clay has been added vs. no clay has been added.

Conclusion

These experiments confirm denitrification activity in OMZ microcosm simulations, and demonstrate a pathway to N_2O production in response to the proposed CCS

method. These experiments did not show a decrease in N_2O produced when clay was added to the microcosms, and over the long term (more than 24 hours), N2O production was indifferentiable between microcosms with and without clay. However, a slight increase in N_2 generated in clay microcosms suggests that the clays may help promote complete denitrification, and therefore over a longer term may decrease N_2O concentrations. Despite the small sample size, the observations made here can guide the development of a more statistically powerful experiment to further discern any differences between these treatments, with a simplified sampling protocol to enable more powerful analysis of these effects. In the meantime, these data show that adding clay minerals to increase organic carbon sinking rate does not increase the climate risks associated with N_2O release by denitrification.

Citations & References

Anderson, Donald M. 1997. "Turning Back the Harmful Red Tide." *Nature* 388 (6642): 513–14. https://doi.org/10.1038/41415.

Bange, Hermann W., S. Wajih A. Naqvi, and L. A. Codispoti. 2005. "The Nitrogen Cycle in the Arabian Sea." *Progress in Oceanography* 65 (2–4): 145–58. https://doi.org/10.1016/j.pocean.2005.03.002.

Barnett, G. R. 1939. "The Use of Sodium Azide in the Winkler Method for the Determination of Dissolved Oxygen." *Sewage Works Journal* 11 (5): 781–87. https://www.jstor.org/stable/25028970.

Bianchi, Daniele, Thomas S. Weber, Rainer Kiko, and Curtis Deutsch. 2018. "Global Niche of Marine Anaerobic Metabolisms Expanded by Particle Microenvironments." *Nature Geoscience* 11 (4): 263–68. https://doi.org/10.1038/s41561-018-0081-0.

Biswas, Shanta, Jannatun Fatema, Tonmoy Debnath, and Taslim Ur Rashid. 2021. "Chitosan–Clay Composites for Wastewater Treatment: A State-of-the-Art

Review." *ACS ES&T Water* 1 (5): 1055–85. https://doi.org/10.1021/acsestwater.0c00207.

Bristow, Laura A., Tage Dalsgaard, Laura Tiano, et al. 2016. "Ammonium and Nitrite Oxidation at Nanomolar Oxygen Concentrations in Oxygen Minimum Zone Waters." *Proceedings of the National Academy of Sciences* 113 (38): 10601–6. https://doi.org/10.1073/pnas.1600359113.

Burd, Emmalina. 2020. *A Study of a Denitrifying Alphaproteobacterium from the Arabian Sea and Its N-Cycling Potential in Sub-Oxic Microzones within the Upper Water Column*. December. http://hdl.handle.net/1893/32516.

Cavan, E. L., M. Trimmer, F. Shelley, and R. Sanders. 2017. "Remineralization of Particulate Organic Carbon in an Ocean Oxygen Minimum Zone." *Nature Communications* 8 (1): 14847. https://doi.org/10.1038/ncomms14847.

Cohen, Yuval. 1977. "Shipboard Measurement of Dissolved Nitrous Oxide in Sea Water by Electron Capture Gas Chromatography." *Analytical Chemistry* 49 (8): 1238–40. https://doi.org/10.1021/ac50016a044.

Devol, Allan H., and Hilairy E. Hartnett. 2001. "Role of the Oxygen-deficient Zone in Transfer of Organic Carbon to the Deep Ocean." *Limnology and Oceanography* 46 (7): 1684–90. https://doi.org/10.4319/lo.2001.46.7.1684.

Halewood, Elisa, Keri Opalk, Lillian Custals, Maverick Carey, Dennis A. Hansell, and Craig A. Carlson. 2022. "Determination of Dissolved Organic Carbon and Total Dissolved Nitrogen in Seawater Using High Temperature Combustion Analysis." *Frontiers in Marine Science* 9 (December): 1061646. https://doi.org/10.3389/fmars.2022.1061646.

Hansen, H. P., and F. Koroleff. 1999. "Determination of Nutrients." In *Methods of Seawater Analysis*, 1st ed., edited by Klaus Grasshoff, Klaus Kremling, and Manfred Ehrhardt. Wiley. https://doi.org/10.1002/9783527613984.ch10.

Hedges, John I., and Richard G. Keil. 1995. "Sedimentary Organic Matter Preservation: An Assessment and Speculative Synthesis." *Marine Chemistry*.

Honjo, Susumu, Steven J. Manganini, Richard A. Krishfield, and Roger Francois. 2008. "Particulate Organic Carbon Fluxes to the Ocean Interior and Factors Controlling the Biological Pump: A Synthesis of Global Sediment Trap Programs since 1983." *Progress in Oceanography* 76 (3): 217–85. https://doi.org/10.1016/j.pocean.2007.11.003.

IPCC. 2022. *Global Warming of 1.5°C: IPCC Special Report on Impacts of Global Warming of 1.5°C above Pre-Industrial Levels in Context of Strengthening Response to Climate Change, Sustainable Development, and Efforts to*

Eradicate Poverty. 1st ed. Cambridge University Press. https://doi.org/10.1017/9781009157940.

Kalvelage, Tim, Marlene M. Jensen, Sergio Contreras, et al. 2011. "Oxygen Sensitivity of Anammox and Coupled N-Cycle Processes in Oxygen Minimum Zones." *PLoS ONE* 6 (12): e29299. https://doi.org/10.1371/journal.pone.0029299.

Karthäuser, Clarissa, Soeren Ahmerkamp, Hannah K. Marchant, et al. 2021. "Small Sinking Particles Control Anammox Rates in the Peruvian Oxygen Minimum Zone." *Nature Communications* 12 (1): 3235. https://doi.org/10.1038/s41467-021-23340-4.

Kuypers, Marcel M. M., Hannah K. Marchant, and Boran Kartal. 2018. "The Microbial Nitrogen-Cycling Network." *Nature Reviews Microbiology* 16 (5): 263–76. https://doi.org/10.1038/nrmicro.2018.9.

Lam, Phyllis, and Marcel M. M. Kuypers. 2011. "Microbial Nitrogen Cycling Processes in Oxygen Minimum Zones." *Annual Review of Marine Science* 3 (1): 317–45. https://doi.org/10.1146/annurev-marine-120709-142814.

Lam, Phyllis, Gaute Lavik, Marlene M. Jensen, et al. 2009. "Revising the Nitrogen Cycle in the Peruvian Oxygen Minimum Zone." *Proceedings of the National Academy of Sciences* 106 (12): 4752–57. https://doi.org/10.1073/pnas.0812444106.

Liu, Hongbin, and Chih-Jung Wu. 2016. "Effect of the Silica Content of Diatom Prey on the Production, Decompositionand Sinking of Fecal Pellets of the Copepod *Calanus Sinicus*." *Biogeosciences* 13 (16): 4767–75. https://doi.org/10.5194/bg-13-4767-2016.

Morrison, J. M., L. A. Codispoti, Sharon L. Smith, et al. 1999. "The Oxygen Minimum Zone in the Arabian Sea during 1995." *Deep Sea Research Part II: Topical Studies in Oceanography* 46 (8–9): 1903–31. https://doi.org/10.1016/S0967-0645(99)00048-X.

Naqvi, S. W. A. 1994. "Denitrification Processes in the Arabian Sea." *Journal of Earth System Science* 103 (2): 279–300. https://doi.org/10.1007/BF02839539.

Paulmier, A., and D. Ruiz-Pino. 2009. "Oxygen Minimum Zones (OMZs) in the Modern Ocean." *Progress in Oceanography* 80 (3–4): 113–28. https://doi.org/10.1016/j.pocean.2008.08.001.

Philippot, Laurent, Janet Andert, Christopher M. Jones, David Bru, and Sara Hallin. 2011. "Importance of Denitrifiers Lacking the Genes Encoding the Nitrous Oxide Reductase for N2O Emissions from Soil: ROLE OF DENITRIFIER

DIVERSITY FOR N2O FLUXES." *Global Change Biology* 17 (3): 1497–504. https://doi.org/10.1111/j.1365-2486.2010.02334.x.

Pocock, K. F., F. N. Salazar, and E. J. Waters. 2011. "The Effect of Bentonite Fining at Different Stages of White Winemaking on Protein Stability: Timing of Bentonite Fining." *Australian Journal of Grape and Wine Research* 17 (2): 280–84. https://doi.org/10.1111/j.1755-0238.2011.00123.x.

Ravishankara, A. R., John S. Daniel, and Robert W. Portmann. 2009. "Nitrous Oxide (N_2 O): The Dominant Ozone-Depleting Substance Emitted in the 21st Century." *Science* 326 (5949): 123–25. https://doi.org/10.1126/science.1176985.

Rounds, S. A., F. D. Wilde, and G. F. Ritz. 2013. "Dissolved Oxygen (Ver. 3.0): U.S. Geological Survey Techniques of Water Resources Investigations." 6.2. *U.S. Geological Survey Techniques of Water Resources Investigations* (Virginia, USA) 9 (A6). http://water.usgs.gov/owq/FieldManual/Chapter6/6.2_v3.0.pdf.

Sauvage, Francois-Xavier, Benoit Bach, Michel Moutounet, and Aude Vernhet. 2010. "Proteins in White Wines: Thermo-Sensitivity and Differential Adsorbtion by Bentonite." *Food Chemistry* 118 (1): 26–34. https://doi.org/10.1016/j.foodchem.2009.02.080.

Shahzadi, Faiza, Xiao-Feng Sun, and Muhammad Sheraz. 2025. "Sustainable Cellulose–Bentonite Composites for Wastewater Treatment." *Materials* 18 (18): 4284. https://doi.org/10.3390/ma18184284.

Sharma, Diksha, Vignesh Gokuladas Menon, Manasi Desai, et al. 2024. "Organoclay Flocculation as a Pathway to Export Carbon from the Sea Surface." *Scientific Reports* 14 (1): 28863. https://doi.org/10.1038/s41598-024-79912-z.

Svensen, C., C. Wexels Riser, M. Reigstad, and L. Seuthe. 2012. "Degradation of Copepod Faecal Pellets in the Upper Layer: Role of Microbial Community and Calanus Finmarchicus." *Marine Ecology Progress Series* 462 (August): 39–49. https://doi.org/10.3354/meps09808.

Thamdrup, Bo. 2012. "New Pathways and Processes in the Global Nitrogen Cycle." *Annual Review of Ecology, Evolution, and Systematics* 43 (1): 407–28. https://doi.org/10.1146/annurev-ecolsys-102710-145048.

Urban, J. L., D. Deibel, and P. Schwinghamer. 1993. "Seasonal Variations in the Densities of Fecal Pellets Produced by Oikopleura Vanhoeffeni (C. Larvacea) and Calanus Finmarchicus (C. Copepoda)." *Marine Biology* 117 (4): 607–13. https://doi.org/10.1007/BF00349772.

Van De Vossenberg, Jack, Dagmar Woebken, Wouter J. Maalcke, et al. 2013. "The Metagenome of the Marine Anammox Bacterium ' *Candidatus* Scalindua Profunda' Illustrates the Versatility of This Globally Important Nitrogen Cycle Bacterium." *Environmental Microbiology* 15 (5): 1275–89. https://doi.org/10.1111/j.1462-2920.2012.02774.x.

Ward, B. B., A. H. Devol, J. J. Rich, et al. 2009. "Denitrification as the Dominant Nitrogen Loss Process in the Arabian Sea." *Nature* 461 (7260): 78–81. https://doi.org/10.1038/nature08276.

Wentworth, W. E., and E. Chen. 1967. "Electron Attachment Mechanisms: Analytical Importance of Temperature and Concentration Variables." *Journal of Chromatographic Science* 5 (4): 170–79. https://doi.org/10.1093/chromsci/5.4.170.

Wentworth, W. E., E. Chen, and R. Freeman. 1971. "Thermal Electron Attachment to Nitrous Oxide." *The Journal of Chemical Physics* 55 (5): 2075–78. https://doi.org/10.1063/1.1676375.

Wentworth, W. E., and R. R. Freeman. 1973. "Measurement of Atmospheric Nitrous Oxide Using an Electron Capture Detector in Conjunction with Gas Chromatography." *Journal of Chromatography A* 79 (May): 322–24. https://doi.org/10.1016/S0021-9673(01)85304-8.

Woebken, Dagmar, Bernhard M. Fuchs, Marcel M. M. Kuypers, and Rudolf Amann. 2007. "Potential Interactions of Particle-Associated Anammox Bacteria with Bacterial and Archaeal Partners in the Namibian Upwelling System." *Applied and Environmental Microbiology* 73 (14): 4648–57. https://doi.org/10.1128/AEM.02774-06.

Wright, Jody J., Kishori M. Konwar, and Steven J. Hallam. 2012. "Microbial Ecology of Expanding Oxygen Minimum Zones." *Nature Reviews Microbiology* 10 (6): 381–94. https://doi.org/10.1038/nrmicro2778.

Wyman, Michael, Sylvia Hodgson, and Clare Bird. 2013. "Denitrifying Alphaproteobacteria from the Arabian Sea That Express *nosZ* , the Gene Encoding Nitrous Oxide Reductase, in Oxic and Suboxic Waters." *Applied and Environmental Microbiology* 79 (8): 2670–81. https://doi.org/10.1128/AEM.03705-12.

Xie, Futai, Zui Tao, Xiang Zhou, Tingting Lv, and Jin Wang. 2019. "Spatial and Temporal Variations of Particulate Organic Carbon Sinking Flux in Global Ocean from 2003 to 2018." *Remote Sensing* 11 (24): 2941. https://doi.org/10.3390/rs11242941.

Xu, Xiaoguang, Yuxuan Yang, Yiwen Zhou, et al. 2025. "Global Patterns and Drivers of Coupling between Anammox and Denitrification Processes

across Inland Aquatic Ecosystems." *Communications Earth & Environment* 6 (1): 23. https://doi.org/10.1038/s43247-024-01980-w.

Yu, Qi, Zhiming Yu, Xiuxian Song, Xihua Cao, Wenbin Jiang, and Yanyang Chu. 2023. "The Synthesis of an Acrylamide Copolymer and Its Synergistic Effects on Clay Flocculation of Red Tide Organisms." *Journal of Environmental Management* 332 (April): 117326. https://doi.org/10.1016/j.jenvman.2023.117326.